Signal Processing for Cloud Studies with the NRL High Power Millimeter Wave WARLOC Radar

WALLACE MANHEIMER

Senior Scientist Fundamental Plasma Processes
Plasma Physics Division

ARNE FLIFLET

Beam Physics Branch
Plasma Physics Division

April 30, 2001

20010518 146

REPORT DOCUMENTATION PAGE

Public reporting burden for this collection of information is estimated to average 1 hour per response, including the time for reviewing instructions, searching existing data sources, gathering and maintaining the data needed, and completing and reviewing the collection of information. Send comments regarding this burden estimate or any other aspect of this collection of information, including suggestions for reducing this burden, to Washington Headquarters Services, Directorate for Information Operations and Reports, 1215 Jefferson Davis Highway, Suite 1204, Arlington, VA 22202-4302, and to the Office of Management and Budget, Paperwork Reduction Project (0704-0188), Washington, DC 20503.

1. AGENCY USE ONLY (Leave Blank)	2. REPORT DATE	3. REPORT TYPE AND DATES COVERED
	April 30, 2001	Interim

4. TITLE AND SUBTITLE	5. FUNDING NUMBERS
Signal Processing for Cloud Studies with the NRL High Power Millimeter Wave WARLOC Radar	

6. AUTHOR(S)

Wallace Manheimer and Arne Fliflet

7. PERFORMING ORGANIZATION NAME(S) AND ADDRESS(ES)	8. PERFORMING ORGANIZATION REPORT NUMBER
Naval Research Laboratory Washington, DC 20375-5320	NRL/MR/6707--01-8545

9. SPONSORING/MONITORING AGENCY NAME(S) AND ADDRESS(ES)	10. SPONSORING/MONITORING AGENCY REPORT NUMBER
Office of Naval Research 800 N. Quincy Street Arlington, VA 22217	

11. SUPPLEMENTARY NOTES

12a. DISTRIBUTION/AVAILABILITY STATEMENT	12b. DISTRIBUTION CODE
Approved for public release; distribution is unlimited.	

13. ABSTRACT (Maximum 200 words)

The WARLOC radar, under final construction at NRL, will be used in part to study cloud dynamics. This radar has at least 3 orders of magnitude more sensitivity than other existing cloud radars at millimeter wavelength. As such it can produce a greatly enhanced image of a cloud. Initial studies will focus on enhanced range resolution in the cloud. This memo outlines the statistics of cloud radar returns as well as the data processing schemes that will be used for enhanced range resolution. These are the use of short radar pulses, the use of pulse compression with a frequency-chirped waveform, and the use of stretch processing for very fine range resolution over a limited region of the cloud.

14. SUBJECT TERMS		15. NUMBER OF PAGES
		27
		16. PRICE CODE

17. SECURITY CLASSIFICATION OF REPORT	18. SECURITY CLASSIFICATION OF THIS PAGE	19. SECURITY CLASSIFICATION OF ABSTRACT	20. LIMITATION OF ABSTRACT
UNCLASSIFIED	UNCLASSIFIED	UNCLASSIFIED	UL

1. Introduction

For radar studies of atmospheric phenomena, one natural decision is whether to operate at long or short wavelength. At long wavelength, the back scattering is typically from atmospheric turbulence, while at short wavelength it is from aerosols. Therefore, in studying clouds at long wavelength (say 10 cm and above), one is actually scattering from the large scale turbulence in the cloud, and one must wonder to what extent the turbulence defines the cloud. However a cloud is actually made up of, and in fact defined by aerosols. In the Rayleigh regime, namely the aerosol radius much less than the radar wavelength divided by 2π, the scattering cross section of the aerosols scales as λ^{-4} where λ is the radar wavelength. Thus at short wavelength, say 3 cm and above, there is very little large scale turbulence, and the scattering is by the aerosols. Since these are what define the cloud, it is natural to perform radar studies of clouds at millimeter wavelengths. However millimeter waves are generally strongly absorbed by the atmosphere. There are two important propagation windows, one at 35 GHz and one at 94 GHz, and both have been used.

There have been a number of studies of clouds with millimeter wave radars [1]. Generally, these radars are restricted to low power, typically an average power of 10 Watts or less. Because of their low power, and short wavelength, they are very typically portable and rather simple to use. For instance they have been fielded on small aircraft for remote sensing of clouds. However because of their low power, they are restricted in what they can detect as regards many important parameters of the cloud. It has long been recognized that higher power millimeter radar could considerably enhance capability [2,3].

The Naval Research Laboratory is now in the process of developing a much more powerful 94 GHz radar. It is called WARLOC [4]. The average power is limited to 10 kW, and the system is portable, although not especially lightweight. The current system is portable on two tractor trailers, one for the radar itself, and one for the power supply. Future upgrades are expected to be transportable on a large aircraft such as an Orion P3. One of the main breakthroughs which make WARLOC possible is the development of a 94 GHz gyroklystron transmitter tube with the required power and bandwidth[5,6]. The waveform generator to the amplifier is capable of producing flexible pulses, nearly arbitrary pulse width and nearly arbitrary frequency chirp. However actual amplitude pulse shape at the output of the gyroklystorn is restricted to be a nearly top hat amplitude distribution. The gyroklystron average power can be as high as 10 kW, peak power as high as 100 kW, and bandwidth is as high as several hundred megahertz. This bandwidth is much more than what is needed for cloud studies, and we do not anticipate using more than 100 MHz for any cloud study. The WARLOC receiver however is limited to a bandwidth of 20 MHz, and this is an important constraint.

WARLOC will be used for a number of possible applications; one of them will be the remote sensing of clouds. With the additional power and sensitivity, we expect WARLOC to

see clouds in many ways in which they have not been seen before. As one of the first experiments, we hope to use the added power to observe the cloud with much greater range resolution. The reason for this choice is that WARLOC appears to be the only remote sensor which can directly examine the interior of a visibly opaque cloud with such fine range resolution. (For a visibly transparent cloud, or for the edges of a visibly opaque cloud, a lidar can achieve similar range resolution.) To do these studies, different data processing techniques will be required on WARLOC. For our initial studies, we will concentrate on post processing of the data. That is the radar will generate raw data of the filter output on tapes. These will produce a first look at the cloud. However this first look will be unsatisfactory in a number of ways. The data will be post processed so as to give a more satisfactory view of the cloud. This memo will discuss some of the signal processing techniques that will be used.

Section 2 discusses the WARLOC radar and the parameters for its cloud study mode of operation. Section 3 discusses the statistical nature of the cloud backscatter for the case of square pulses with no frequency chirp. With the 20 MHz receiver bandwidth, the shortest transmitted pulse that can be processed is 50 ns, so the range resolution will be about 8 meters. This is considerably less than what can be resolved with the lower power millimeter radar systems. Section 4 discusses improved range resolution with a frequency chirped pulse with both a square amplitude pulse and a Gaussian amplitude pulse. With pulse compression, one effectively packs the energy of say a 10 μs pulse into 50 ns, thereby greatly increasing the sensitivity of the radar. However with pulse compression, there is the possibility of range sidelobes and these must be reduced as much as possible. For instance if there is a large cross section portion of the cloud next to a small cross section portion, the range sidelobes from the large cross section part may swamp the main signal from the small cross section part. As we will see, a Gaussian amplitude profile greatly reduces this problem; but unfortunately, WARLOC is constrained to transmit only a square amplitude pulse.

Section 5 discusses ways to reduce the sidelobes with an additional Gaussian filter or with a nonlinear frequency chirp. The sidelobes can be significantly reduced in this way, but at the expense of some range resolution. Here the receiver bandwidth limit of 20 MHz really makes itself felt. In Section 6 we discuss stretch processing. This allows us to use the full transmitter bandwidth to obtain very fine range resolution, but only in a small part of the cloud. With stretch processing, WARLOC will be able to obtain roughly one and a half meter range resolution over about 75 meters of the cloud. Note that the range resolution of the radar is determined by the speed of the processor, not by the bandwidth of the gyroklystron, which is well in excess of 100 MHz. Thus relatively straightforward and inexpensive enhancements to WARLOC can be achieved by increasing the processor rate to say 100 MHz.

2. Cloud Studies with WARLOC

We begin here with a simple examination of the pulse requirements for a cloud radar. In any pulsed radar, the time between pulses T must be long enough that the return from the

furthest target on the $(n-1)^{st}$ pulse does not interfere with the return from the closest target on the nth pulse. This then gives the condition for range ambiguity. The greater the pulse separation, the less of a concern range ambiguity becomes. In a pulsed Doppler radar, the motion of a target causes a phase change from one pulse to the next. However this phase change must be less than 2π in order to avoid velocity ambiguity or blind speeds. The condition to avoid both range and Doppler ambiguity in a pulsed radar is given by

$$2R_{max}/c < T < c/2f_o v_{max} \qquad (1)$$

where R_{max} is the maximum target range, v_{max} is the maximum target velocity, and f_o is the radar frequency. As the frequency increases, the second inequality become harder to satisfy. Another issue is the minimum range or dead time of the radar. Since the radar cannot receive while it is transmitting, the minimum range at which a target can be detected is $c\tau/2$, where τ is the pulse time.

The WARLOC radar is now in its final construction phase at NRL. Once some initial tests are made on base, the entire radar will be transported to NRL's field cite at Cheasepeake Bay Division (CBD), and most of the radar tests, of both clouds and other targets will done at CBD. It is anticipated that WARLOC will be set up at CBD in about April or May of 2001. Once set up there, support exists to keep the radar operational there for about 2 years, during which time it will examine clouds and other targets.

We now consider WARLOC's operation in the cloud sensing mode. Its initial task will be to examine a cloud with finer range resolution. This can be done in either of two ways. The first is to transmit short pulses, the second to transmit long pulses with a frequency chirp and then pulse compress. Some basic approximate parameters: maximum average power: 10 kW, peak power: 100 kW. If we consider 10 μsec pulses, maximum reprate = 5,000 Hz, so as not to overly stress the system, the range ambiguity distance is 30 km, and minimum distance to target is 1.5 km. These numbers are probably satisfactory for most initial applications. As an option, we might want to consider working with shorter pulses, maybe 1-3 μsec in some cases, but this would probably mean reducing the average power by this factor.

Most of the data would be taken in a pulse compressed mode. Since the receiver processor is limited to 20 MHz, this means a range resolution of 7.5 meters, corresponding to about a 50 nsec pulse. We would send out a signal with a 20 MHz chirp and process through a Gaussian filter. We would want integrated sidelobes down by 30 db, and this closest sidelobe down by 40 db.

There are two alternate modes in which we would want to operate the radar. The first is to simply transmit a 50 nsec pulse with no frequency chirp. This would degrade the average power, but it would have the advantage of operating with no problem from range sidelobes.

Operating the radar in this mode would still give a large enhancement over typical low power cloud radars which have peak powers of about 1 kW.

The second operating regime would be to examine a small part of an extended cloud at much greater range resolution by using stretch processing. This allows the full bandwidth of the transmitter to be used, but to still process at 20 MHz in the receiver. Let us imagine the transmitter bandwidth as 100 MHz, so that the range resolution becomes 1.5 meters.

Let us consider other capabilities we hope to bring to bear. One other capability which WARLOC and only WARLOC would have would be to examine a cloud in three dimensions in space and time. For instance we could examine the full dynamics of a cloud as it drifted by. For this it would be important for the radar to have 2π sterradian beam steering capability. Displaying the three dimensional data collected would entail image processing and display technology which we have not addressed at this time.

Depolarization by non spherical droplets (especially by ice clouds) is an important physical process in cloud radar systems. While WARLOC will not have full polarametric capability (i.e. vary the polarization on the transmit and the receive), it will be able to process a received signal with arbitrary polarization.

3 Statistical properties of cloud returns from a sequence of square pulses

Let us say that the radar transmits a pulse given by

$$T(t) = \mathrm{Re}\, H(t) \exp - i\omega_0 t \tag{2}$$

where H is a complex amplitude function which designates both an amplitude profile and frequency chirp. The pulse is backscattered by a random ensemble of scatterers, where index i denotes the individual scatterer. Then the returned pulse is denoted by

$$\mathbb{R}(t) = \sum_i \xi_i \, \mathrm{Re}\, H\left\{ t - 2\left[\frac{R_i + v_i t}{c} \right] \right\} \exp - i\omega_0 \left\{ t - 2\left[\frac{R_i + v_i t}{c} \right] \right\} \tag{3}$$

Here R_i is the position of the scatterer at time t=0, v_i is its velocity, and ξ_i denotes the strength of the scatterer. It is proportional to the square root of its cross section divided by the range squared.

The most fundamental data that the radar system gives is to take the returned signal and pass it through a low pass filter to give a filtered signal

$$\mathbb{R}_f(t) = \sum_i \xi_i \, \text{Re} \, H \left\{ t - 2 \left[\frac{R_i + v_i t}{c} \right] \right\} \exp{-2i \frac{\omega_0 (R_i + v_i t)}{c}} \tag{4}$$

Thus data processing concerns how to deal with $\mathbb{R}_f(t)$ so as to obtain the desired information. One common way to process this signal is to sent it through a matched filter[7]. The matched filter selects a time, or series of times denoted t_j and forms the time or Fourrier domain integral

$$M_j = \int_{-\infty}^{\infty} dt \mathbb{R}_f(t) H^*(t_j - t) \equiv \frac{1}{2\pi} \int_{-\infty}^{\infty} d\omega \mathbb{R}_f(\omega) H^*(\omega) \exp{-i\omega t_j} \tag{5}$$

The Fourrier and inverse Fourrier transforms of any square integrable function are written as

$$Z(t) = \int_{-\infty}^{\infty} d\omega Z(\omega) \exp{-i\omega t} \qquad Z(\omega) = \frac{1}{2\pi} \int_{-\infty}^{\infty} dt Z(t) \exp{i\omega t} \tag{6}$$

The matched filter response both maximizes the signal to noise for the case of white noise, and also does the pulse compression where H(t) includes a frequency chirp. We can also denote reference range or sequence of reference ranges as $R_j = ct_j/2$. While the integral in the Fourrier domain is shown as being from minus infinity to infinity, in reality, the maximum frequency is limited by the sampling rate of the receiver. For WARLOC in the standard mode of operation, this sampling rate is 20 MHz, so for realistic pulses, the factors in the frequency integrand of Eq. (5) are essentially zero , since the WARLOC receiver has filters which provide for hard frequency cutoffs at the edges of the processing bandwidth .

Let us assume that τ is sufficiently small that the Doppler shift in frequency within the pulse is not significant. For the case of a square pulse of pulse length τ with no frequency chirp, the time domain integral is especially simple. It is

$$M_j = \sum_i \xi_i \tau_i \exp{i\psi_i} \tag{7}$$

where

$$\tau_i = 0 \qquad \text{for } 2R_i/c > t_j \tag{8a}$$

$$\tau_i = t_j - 2R_i/c \qquad \text{for } t_j - \tau < 2R_i/c < t_j \tag{8b}$$

$$\tau_i = 2R_i/c - t_j + 2\tau \qquad \text{for } t_j - 2\tau < 2R_i/c < t_j - \tau \qquad (8c)$$

$$\tau_i = 0 \qquad\qquad \text{for } 2R_i/c < t_j - 2\tau \qquad\qquad (8d)$$

and

$$\psi_i = \frac{2\omega R_i}{c}\left(1 + \frac{2v_i}{c}\right) \qquad\qquad (9)$$

At the boundary between the second and third region, τ_i has its maximum value of τ. At $|R_i - R_j| = c\tau/2$, it falls to half its value and we define this as the range resolution. However this is not aprecise definition because targets outside of this range can also contribute to the filter response. However if $|R_i - R_j| > c\tau$, $M = 0$, so targets far away do not contribute no matter how large their cross section. Thus the range resolution is determined by the pulse time for a pulse with no frequency chirp. Let us consider the 20 MHz receiver bandwidth constraint here. If the received signal is digitized, and the nature of the digitizer is to average over successive 50 ns time intervals, then the A:D converter *is* a matched filter.

We assume that the droplet positions are uncorrelated so that ψ_i is a random phase. Since the radar typically ultimately uses a square law detector, we find that

$$|M_j|^2 = \left\{ \sum_i |\xi_i|^2 \tau_i^2 + \sum_{i \neq k} \xi_i \xi_k \tau_i \tau_k \exp i(\psi_i - \psi_k) \right\} \qquad (10)$$

The first term in the summation on the left hand side of Eq. (10) is simply the sum of the power scattered from each droplet. This is the coherent response. For the simple case of all ξ's being equal and the droplets distributed uniformly in the range cell, the coherent response is

$$|M_j|_{coh}^2 = \frac{2}{3}N\tau^2\xi^2 \qquad\qquad (11)$$

where N is the number of droplets in the range cell. However, the second term of Eq. (10), which ensemble averages to zero over random phases, actually constitutes a significant, i.e. nearly of order unity fluctuation in any realization of the ensemble. Now let us get the magnitude squared of the ensemble average of the error. It is

$$\left| \left| \Delta M_j \right|^2 \right|^2 = \left\langle \left\{ \sum_{i \neq k, l \neq m} \xi_i \tau_i \xi_k \tau_k \xi_l \tau_l \xi_m \tau_m \exp i \left(\psi_i - \psi_k + \psi_l - \psi_m \right) \right\} \right\rangle \qquad (12)$$

The ensemble average above vanishes unless i=l and k=m. Assuming that the number of droplets is large compared to unity, we find

$$\left| \left| \Delta M_j \right|^2 \right|^2 = \sum_{i,k} \left| \xi_i \right|^2 \left| \xi_k \right|^2 \tau_i^2 \tau_k^2 \equiv \frac{4}{9} N^2 \tau^4 \left| \xi \right|^4 \qquad (13)$$

where on the right hand equation in Eq. (13) we have assumed once more that all ξ's are the same, that the droplets are distributed uniformly in the range cell, and N is the total number of droplets in the volume. One measure of the relative error is then

$$\frac{\sqrt{\left| \left| M_j \right|_{coh}^2 \right|^2 + \left| \left| \Delta M_j \right|^2 \right|^2} - \left| M_j \right|_{coh}^2}{\left| M_j \right|_{coh}^2} = 0.41 \qquad (14)$$

or the signal is 3.8 db above the noise by this measure. Another measure [8],

$$\frac{\left\langle \left| M_j^2 \right| \right\rangle - \left\langle \left| M_j \right|^2 \right\rangle}{\left\langle \left| M_j \right|^2 \right\rangle} = .27 \qquad (15)$$

gives a similar result. With this measure, the signal is 5.7 db above the noise. Either way, the errors are almost of order unity.

Now let us consider how the noise is reduced by multiple pulses. Furthermore, if we consider multiple pulses, there are phase changes from pulse to pulse due to the droplet motion. We now consider how these effects are treated. Let us say we transmit a total of P pulses, and let p be an index which denotes a pulse in this sequence. Furthermore, let us say that during the time of the total pulse train, PT, the droplets can move long distances compared to the radar wavelength λ, but cannot move far compared to a range cell. In this case, the matched filter response acquires an additional index p

$$M_j(p) = \sum_i \xi_i \tau_i \exp i \psi_i(p) \qquad (16)$$

7

where

$$\psi_i(p) = \frac{2\omega R_i}{c}\left(1 + \frac{2v_i}{c}\right) + \frac{2\omega v_i pT}{c} \tag{17}$$

Note that $M_i(p)$ now has an additional phase factor which varies from pulse to pulse according to the droplet velocity. This phase change is what provides the velocity, or Doppler information in a pulsed Doppler radar. However let us first see how the multipulse operation reduces the statistical errors. To do so, introduce another variable z, which is the Fourrier transform variable to p

$$f(z) = \sum_{p=0}^{P-1} f(p)\exp\frac{2\pi i p z}{P} \tag{18}$$

Now form the summation

$$S_j = \sum_{z=0}^{P-1}\left|M_j(z)\right|^2 = \sum_{z=0}^{P-1}\sum_{p=0}^{P-1}\sum_{q=0}^{P-1}\tau_i\tau_k\xi_i\xi_k\sum_{i,k}\expi\left[\psi_i - \psi_k + \frac{2\omega T}{c}\left(pv_i - qv_k\right) + \frac{2\pi(p-q)}{P}\right] \tag{19}$$

Where to simplify, we have once more assumed that all ξ_l's are the same. The summation over z simply gives $P\delta_{p,q}$, and then the summation over q reduces then to a summation over p where p = q is taken in the summation. Once more, we can break the summation into a coherent and incoherent part, where p = q, and $p \neq q$. The coherent term is simply P times the previous result for the coherent term, Eq. (11).

The incoherent term ensemble averages to zero, but we would like to get an idea of its average magnitude. As before, square it and take its magnitude. We find

$$\left|\Delta S_j\right|^2 = \sum_{p=0}^{P-1}\sum_{q=0}^{P-1}\sum_{i\neq k}\tau_i^2\tau_k^2\left|\xi_i\right|^2\left|\xi_k\right|^2\expi\left[\frac{2\omega T}{c}(p-q)(v_i - v_k)\right] \tag{20}$$

Now replace the summations by integrals over distribution functions.

$$\sum_i = N\int dv_i f(v_i) \tag{21}$$

and as before, assume the ξ's are all equal and the droplets are distributed uniformly to rewrite Eq. (20) as

8

$$\left| \Delta S_j \right|^2 = \frac{4}{9} (\tau \xi)^4 N^2 \sum_{p=0}^{P-1} \sum_{q=0}^{P-1} \iint dv d\Delta v f(v) f(\Delta v | v) \exp i \left[\frac{2\omega T}{c} (p-q) \Delta v \right] \quad (22)$$

The result then depends on the distribution of droplet velocities and the correlation of droplet velocities with one another in the range cell. If we make the simple assumption the distribution of Δv is a Maxwellian with thermal velocity v_t independent of v,

$$f(\Delta v | v) = \frac{1}{\sqrt{2\pi} v_t} \exp - \left[\frac{\Delta v}{2 v_t} \right]^2 \quad (23)$$

we find that

$$\left| \Delta S_j \right|^2 = \frac{4}{9} (\tau \xi)^4 N^2 \sum_{p=0}^{P-1} \sum_{q=0}^{P-1} \exp - \left[\frac{2\omega T}{c} (p-q) v_t \right]^2 \quad (24)$$

If $p = q$, the terms are as in the calculation of the coherent part. There are P of these terms. The terms with $p \neq q$ are all reduced by the exponential factor, and their contribution becomes very small if $p - q > c/(2\omega T v_t)$. If we further simplify by setting the exponential equal to unity if the inequality is violated, and equal to zero of the inequality is satisfied, we find approximately

$$S_j \propto \frac{2}{3} NP (\tau \xi)^2 \left[1 + \frac{c}{2\omega P T v_t} \right]^{1/2} \quad (25)$$

where the first term in the square brackets represents the coherent term, and the second term denotes the approximate magnitude of the statistical error. Thus over a long series of pulses, the relative statistical fluctuations to the signal get smaller and smaller. In order for the fluctuations to die away, the total length of the pulse train, PT must be very long compared to the time for the particles to move apart from one another by a radar wavelength. Of course this is to be expected, since it is generally assumed that an ensemble average is in some sense equivalent to a time average. Our calculation quantifies this for the cloud. It shows that as long as there is sufficient velocity spread to the droplets, the time average approaches the ensemble average as the reciprocal of the total time PT. Since τ and P are known, a sequence of P pulses then gives a reasonably accurate estimate of $N\xi^2$, effectively the sum of the scattering cross sections of all the droplets.

Let us now consider how to retrieve the Doppler information. Of course we cannot get the velocity of every droplet, so one must define moments of the droplet distribution function. Let us consider the quantity $z|M_j(z)|^2$. Retaining only the coherent response, and setting the summation over particles to an integral over a distribution of droplet velocities, we find that this expression can be manipulated into the form

$$z|M_j(z)|^2 = \frac{2}{3}(\tau\xi)^2 N\int dv f(v)z \frac{\sin^2 P\left(\frac{\omega vT}{c}+\frac{\pi z}{P}\right)}{\sin^2\left(\frac{\omega vT}{c}+\frac{\pi z}{P}\right)} \tag{26}$$

If P is large, the ratio of the two sins is sharply peaked near $[(\omega vT/c)+(\pi z/P)]=0$. At this point, the value of the ratio is P^2, and the width of the function is about π/P. If the thermal width of $f(v)$, v_t is much larger than $\pi c/\omega T$, then the distribution function may be evaluated at $v=-\pi z c/\omega T$ and taken out of the integral. Then we find

$$z|M_j(z)|^2 = \frac{2}{3}(\tau\xi)^2 Nz\pi P\frac{c}{\omega T}f(v=-\pi z c/\omega T) \tag{27}$$

Since P and τ are known, and $N\xi^2$ can be obtained from Eq. (11) an approximation to the droplet velocity distribution can then be obtained. (Of course for cases where the velocity is positive, z does not have to go from 0 to P-1, but can be taken from for instance –P/2 to P/2 – 1). However the correction to Eq. (27) from the incoherent return is, as before, nearly of order unity, so the distribution of droplet velocities has rather large statistical fluctuations in any realization of the ensemble. If there is time to do many sequences of P pulses before the droplets move out of the range cell, these statistical fluctuations can be reduced as before.

It may not be necessary to obtain the entire velocity distribution function for the droplets but only a moment of the distribution. Summing Eq. (27 over z, and approximating the summation over z by an integral over v, we find

$$\sum_z z|M_j(z)|^2 = (\tau\xi)^2 NP\frac{\omega T}{\pi c}\int dv v f(v) \tag{28}$$

Since we are now summing over z, the statistical fluctuations will be much smaller as was the case of Eq. (25). The right hand side is a product of known quantities times the average velocity of the droplets.

4 Improved range resolution by pulse compression

A standard technique in radar signal processing is to use a chirped pulse. For instance, let us assume the envelope of the transmitted pulse is

$$H(t) = Q(t)\exp{-i\omega'(t-\tau/2)^2} \tag{29}$$

where Q is top hat function, equal to unity between 0 and τ, and equal to zero otherwise. Now let us calculate the matched filter response for a single target at range R_i and a time displacement of t_j. There are 4 regimes for the time integral in Eq. (5). These are,

I: $2R_i/c + \tau < t_j$, II: $t_j < 2R_i/c + \tau < t_j + \tau$, III: $t_j < 2R_{i<}/c < t_j + \tau$, IV: $\tau + t_j < 2R_i/c$

In cases I and IV, the matched filter response is zero because the two Q functions do not overlap. For case II, we find the matched filter response is

$$M_j = \exp{-(2iR_i\omega/c)}\frac{\sin\omega'\left(t_j - \dfrac{2R_i}{c}\right)\left(\dfrac{2R_i}{c} + \tau - t_j\right)}{\omega'\left(t_j - \dfrac{2R_i}{c}\right)} \tag{30}$$

while for Case III we find

$$M_j = \exp{-(2iR_i\omega/c)}\frac{\sin\omega'\left(t_j - \dfrac{2R_i}{c}\right)\left(\tau + t_j - \dfrac{2R_i}{c}\right)}{\omega'\left(t_j - \dfrac{2R_i}{c}\right)} \tag{31}$$

This matched filter response is shown in Fig. (1) for what we call our standard WARLOC pulse. This is a 10 μs pulse with a linear frequency chirp going from −10 MHz to +10 MHz in that time. In Fig. (1A) is the magnitude squared of the matched filter response for the central 2 μs, Fig. (1B) shows the expanded scale for the entire 20μs of overlap. We define the range resolution as the time between the 3 dB points in the main lobe of the matched filter response, which is 48 ns. This corresponds to a range resolution of 48 ft.

Consider the case of a target near the center of the range cell, $t_j \approx 2R_i/c$. If $t_j = 2R_i/c$, the magnitude of the filter response is τ, and it falls to zero at $\omega'\tau\left(t_j - 2R_i/c\right) = \pi$. But $\omega'\tau$

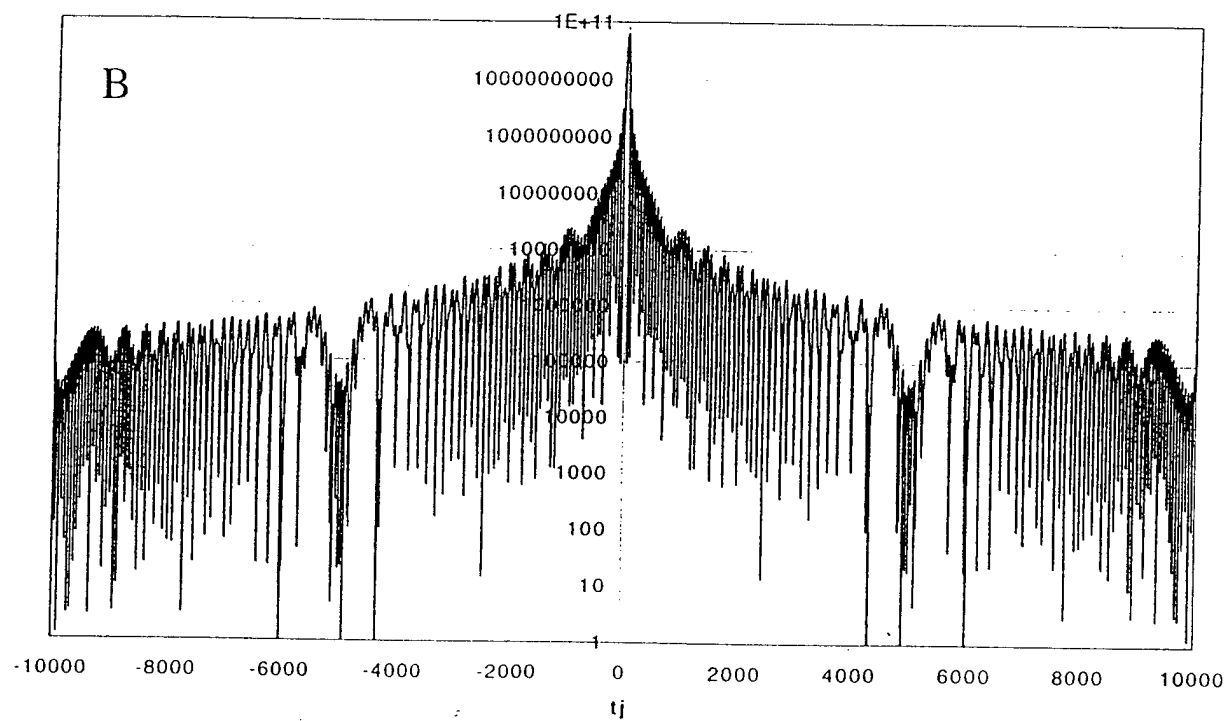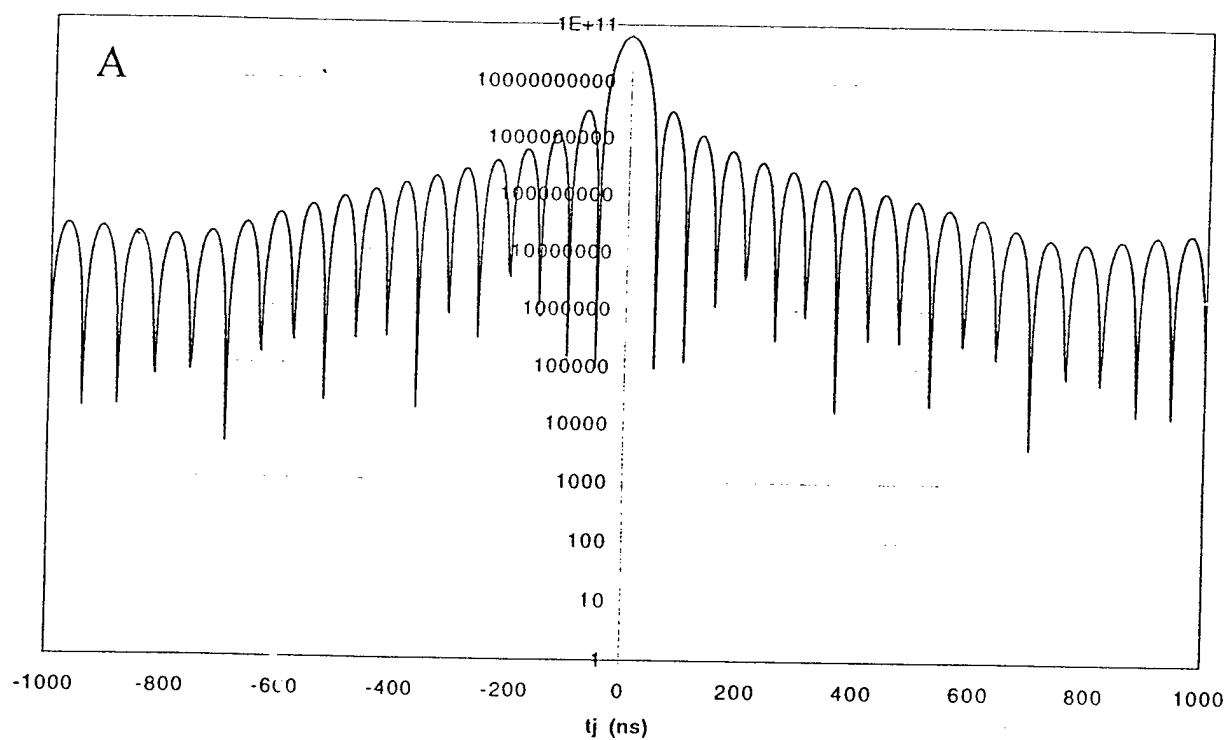Figure 1.   Matched filter response for the standard WARLOC pulse, A) central 2 μs, and B) the entire 20μs overlap.

is the change in angular frequency over the course of the pulse. However, if the range is such that $\omega'\tau\left(t_j - 2R_i/c\right) = 3\pi/2$, the filter again is at a relative maximum, although it is smaller than the central maximum. These are the range sidelobes. For a square law detector, this maximum is smaller than the central maximum by a factor of $4/9\pi^2$, or by about 13 db. the integrated sidelobes are down by 9.3 dB. For many circumstances, this is not satisfactory. For instance if there is a large target near a small target, the range sidelobe of the large target may exceed the return of the small target.

We now discuss one way of minimizing these sidelobes. One classic technique is to use a Gaussian, rather than a top hat amplitude envelope. Let us say that the frequency chirp is as given in Eq. (29), but the amplitude is given by $\exp\text{-}(t/\tau)^2$. The Fourrier transform of the Gaussian also extends to infinity, but the amplitude at large frequency falls off very fast. Whether this can be accommodated by the 20 MHz receiver bandwidth depends on the details of the receiver filter.

It is not difficult to do the time integral in Eq. (5) and find the filter response

$$M_j = \sum_i \sqrt{\frac{\pi}{2}}\xi_i\tau_i \exp i\psi_i \exp-\left[\left(R_i - R_j\right)^2\left(\frac{2}{c^2\tau^2} + \frac{8\omega'^2\tau^2}{c^2}\right)\right] \tag{32}$$

There are two contributions to the range resolution, one from the pulse time (the first term in the second bracket in the exponent), and one from the total frequency chirp (the second term). Usually the total frequency chirp is much larger than the reciprocal of the pulse width, so the range resolution is determined by the frequency spread in the pulse. Furthermore, because of the Gaussian structure of the filter response, the sidelobes are substantially reduced. For instance a target four range cells away contributes only exp-16 times as much as a target in the center of the range cell. Thus the use of Gaussian pulses is one way of reducing the range sidelobes in a pulse compressed radar. However in WARLOC, this is very difficult to do. If the waveform generator were to generate a Gaussian pulse, there are many amplifiers between it and the output pulse, including the gyroklystron. All or many of these are run at saturation, so that in reality, the only choice for an amplitude waveform in WARLOC is a top hat. In the next two sections, we will discuss how range sidelobes may be reduced in this case.

5. Sidelobe reduction for practical radar pulses

We have seen that a Gaussian pulse amplitude reduces the sidelobes. However between the waveform generator and final output pulse in WARLOC, there are several amplifiers run at saturation. Thus a top hat, or nearly top hat pulse amplitude is the only practical way to

operate WARLOC, and we would like to reduce the range sidelobes subject to this constraint. Here we look at additional Gaussian filtering, and then very briefly discuss the use of a nonlinear chirp [9. We first consider a linear chirp, but a non-matched filter in the receiver. We consider the filter in the Fourrier domain. To start, we would like to calculate the Fourrier transform of the radar pulse

$$H(\omega) = \frac{1}{2\pi} \int_{-\tau/2}^{\tau/2} dt \exp-i\left(\omega't^2 + \omega t\right) \tag{33}$$

There is no simple analytic expression for the above integral, but one can use a saddle point approximation. There is a saddle point at $t = \omega/2\omega'$. First consider the case of

$$-\frac{\tau}{2} < \frac{\omega}{2\omega'} < \frac{\tau}{2} \tag{34}$$

In this case the saddle point is along the path of integration, and the path of integration may be deformed as shown in Fig. (2). With respect to an origin at the saddle point, the integrand is exponentially small in the second and fourth quadrant, and exponentially large in the first and third. The path shown as II is the saddle point path, and the paths I and III are the other parts of the contour. The saddle point contribution is given approximately by

$$\sqrt{\frac{\pi}{\omega'}} \exp i \frac{\omega^2}{4\omega'} \tag{35}$$

while the integral along path III can be written as

$$\exp i \frac{\omega^2}{4\omega'} \exp-\omega'\left[\frac{\tau}{2} - \frac{\omega}{2\omega'}\right]^2 \int_0^{\tau/2 - \omega/\omega'} d\zeta \exp\left[\omega'\zeta^2 + 2i\omega'\left(\frac{\tau}{2} - \frac{\omega}{2\omega'}\right)\zeta\right] \tag{36}$$

A rough measure of the magnitude of the integral in Eq. (36) is given by the maximum value of the integrand times the size of the region over which it has that value. This is determined by the fall off of the exponential, or the length of the oscillation. Both of these determine a region of about the same size. We find that the ratio of the integral along path III to the saddle point contribution is about
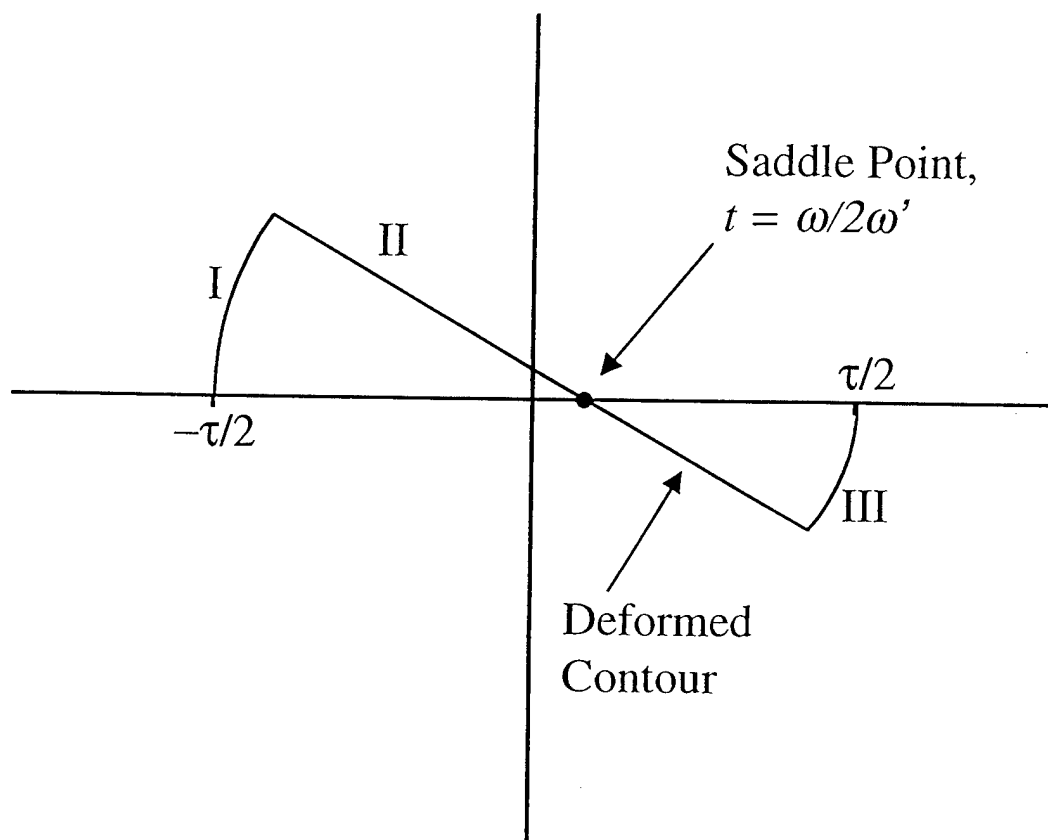
Figure 2. The original contour for the evaluation of H(ω) in Eq. 33, and a contour deformed so as to pass through the saddle point.

$$\frac{\int_{\text{III}}}{\int_{\text{II}}} \approx \frac{1}{\sqrt{\omega' \tau^2}} \qquad (37)$$

That is the saddle point contribution is larger by about the square root of the total chirp phase. The magnitude of the saddle point contribution is independent of frequency, so the magnitude of the Fourrier transform of the signal is roughly independent of frequency if Eq. (34) is satisfied.

Now let us consider the transform for frequency outside the range defined by Eq. ()34. The path cannot be deformed into one where the dominant contribution is from the saddle point. Since the integrand is then everywhere rapidly oscillating, we expect that the Fourrier transform of the signal will be very small for ω outside the range determined by Eq. (34). Shown in Fig (3) is a numerical calculation of the square of the magnitude of the Fourrier transform of the signal for the standard WARLOC waveform. Clearly, a top hat function is also a reasonable approximation to the Fourrier transform of the radar pulse.

From the numerical calculation of the Fourrier transform of the signal, we can do the integral in the Fourrier domain in Eq. ()5 to get the filter response as a function of t_j where now t_j in Eq. (5) is understood as being the time delay between the filter time origin and the return time of the signal. That is $t_j = 2(R_i - R_j)/c$.

The sidelobes can be reduced by multiplying the matched filter response $H^*(\omega)$ by a Gaussian filter,

$$f_G(\omega) = \exp - \frac{\omega^2}{\omega_G^2} \qquad (38)$$

and using this as the filter function. Since the Gaussian has smooth wings, the sidelobes are greatly reduced. Shown in Fig. (4A) is the non matched filter response, $|M_{jn}|^2$ as a function of t_j for the case of $\omega_G = 5$ MHz for the central 2μs, and in Fig. (4B) is shown the result for the entire 20 μs of overlap. Clearly the sidelobes are reduced by a considerable amount. However there is some penalty in range resolution.

Since the filter is not matched, the sensitivity is lower than optimal. Let us define the filter efficiency η, for a target at the center of the range cell as
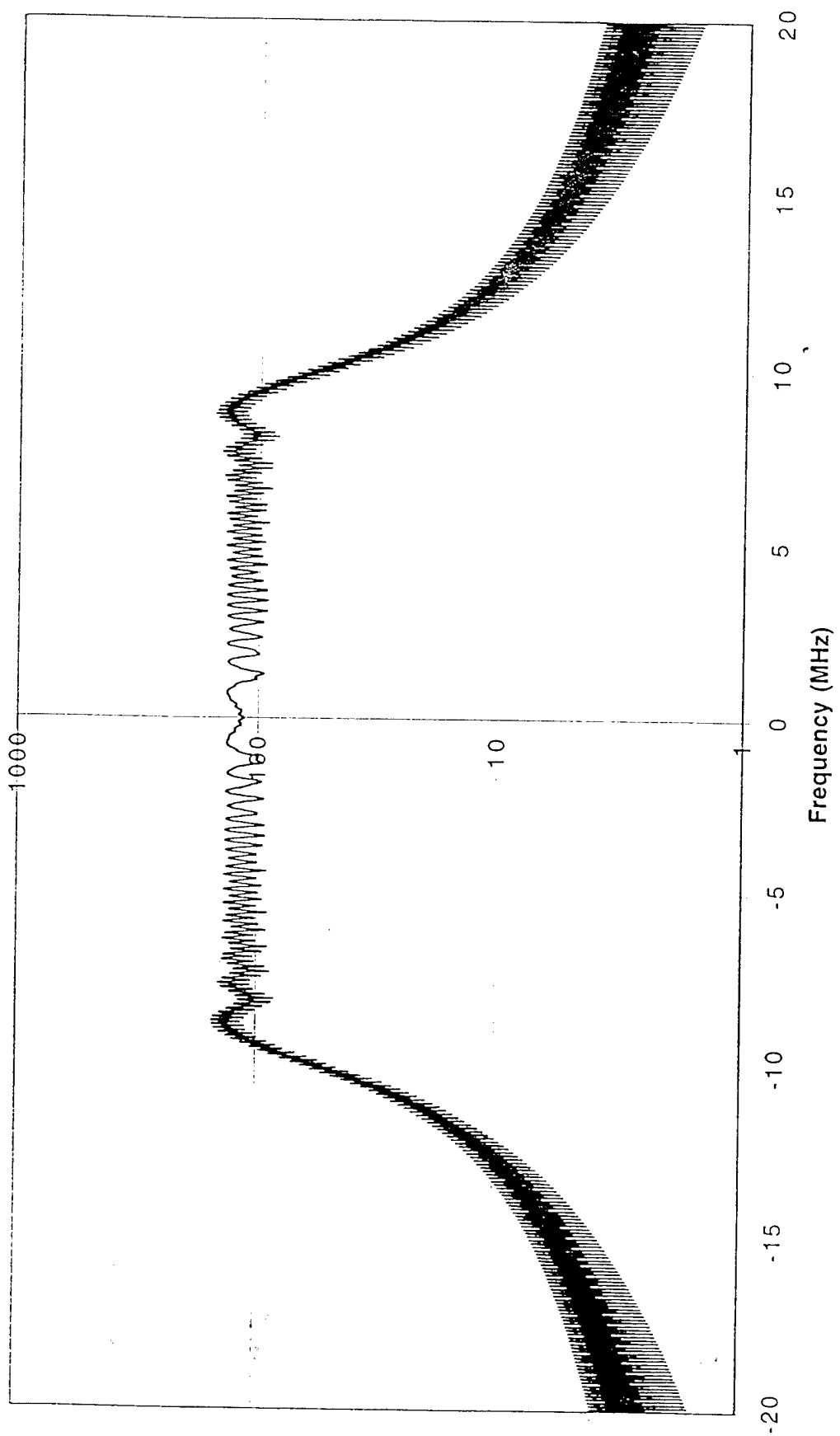
Figure 3. The frequency spectrum of the square pulse with linear chirp for the standard WARLOC pulse.
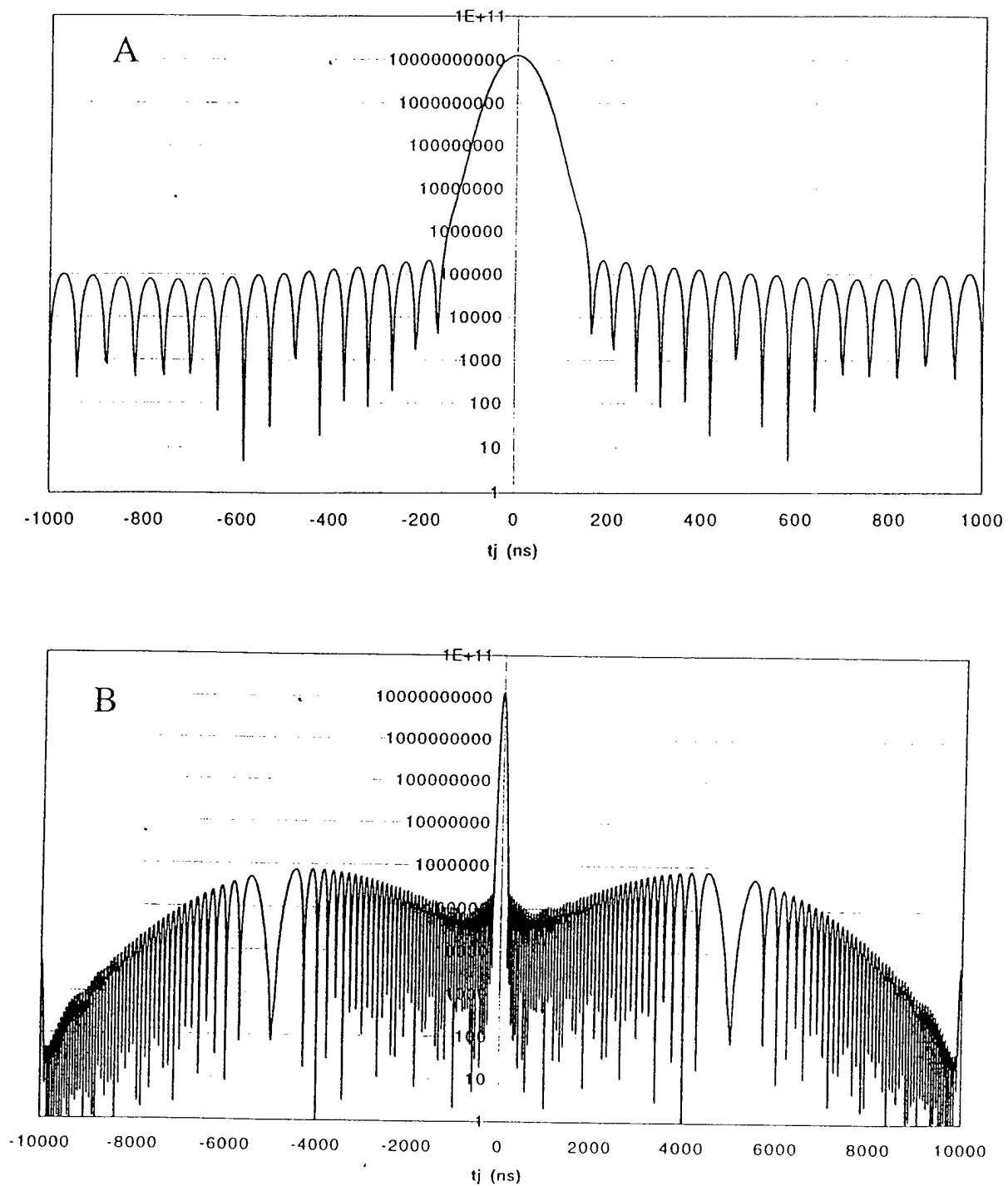
Figure 4.   Filter response for the standard WARLOC pulse with an added Gaussian filter with $f_G = 5$ MHz, A) central 2 μs, and B) the entire 20 μs of overlap.

$$\eta = \frac{\left|\int d\omega R^*(\omega) f_G(\omega) R(\omega)\right|^2}{\int d\omega |R^*(\omega) f_G(\omega)|^2 \int d\omega |R(\omega)|^2} \qquad (39)$$

By the triangle inequality, it maximizes at unity for a matched filter. In Table (1) are enumerated the range resolution in ns, the integrated sidelobes, and the efficiency for the matched filter as well as for the additional Gaussian filter with values of ϕ_G of 5, 7.5 and 10 MHz. We consider mostly the 5 MHz filter which appears to be a good compromise between sidelobe reduction, range resolution, and efficiency.

It is apparent form Fig. (4B), that the sidelobes are enhanced around the time where the center filter pulse overlaps the edge of the received pulse. We interpret this as a consequence of the sharp cutoffs of the top hat function. In practice, the edges of the pulses will be rounded somewhat. The transmitted pulse will be rounded because the turn on time of the gyroklystron is not instantaneous, but has some non zero turn on and turn off time. It may be that it is possible to exercise some control of the turn on and turn off of the transmitted pulse. The filter pulse, of course can round the edges at will.

We investigate here the effect of rounded edge pulses. We model the rounding function $R(t)$ as

$$R(t) = 0.5\left(1 + \cos\frac{\pi(t - T_e)}{T_r}\right) \qquad (40)$$

at the end of the pulse, with an analogous function at the beginning. Here T_e end time of the top hat pulse shape, and T_r is the time for the pulse to go to zero. Since the filter response in the central maximum is not strongly dependent on the precise pulse edge, the efficiency and range resolution are basically unaffected. However the distant sidelobes are reduced. Shown in Fig. (5) is the filter response for the 5 MHz Gaussian filter with a pulse turn time of 200 ns in both the transmitted pulse and filter. Clearly the distant sidelobes are considerably reduced. In Table (2) are shown the sidelobe reduction for the 5 MHz Gaussian filter for various turn on and turn off times for the transmitted pulse $T_r(T)$, and filter pulse, $T_r(F)$. While ordinarily these would be the same, they do not have to be. If the transmitter is constrained to a maximum $T_r(T)$, the sidelobes can still be reduced by taking a larger value of $T_r(F)$.

Another way of reducing the sidelobes is by using a nonlinear chirp with a matched filter. A we have seen from our saddle point calculation, the magnitude of the Fourrier transform of the waveform is proportional to the reciprocal of the time the pulse is at each frequency. For the linear chirp we have been discussing, the frequency is uniformly swept, so the Fourrier transform is nearly a top hat function. This transform can be rounded off by sweeping faster at the frequency extreme. In Ref. (9), the "circle ϕ" chirp is used, which is
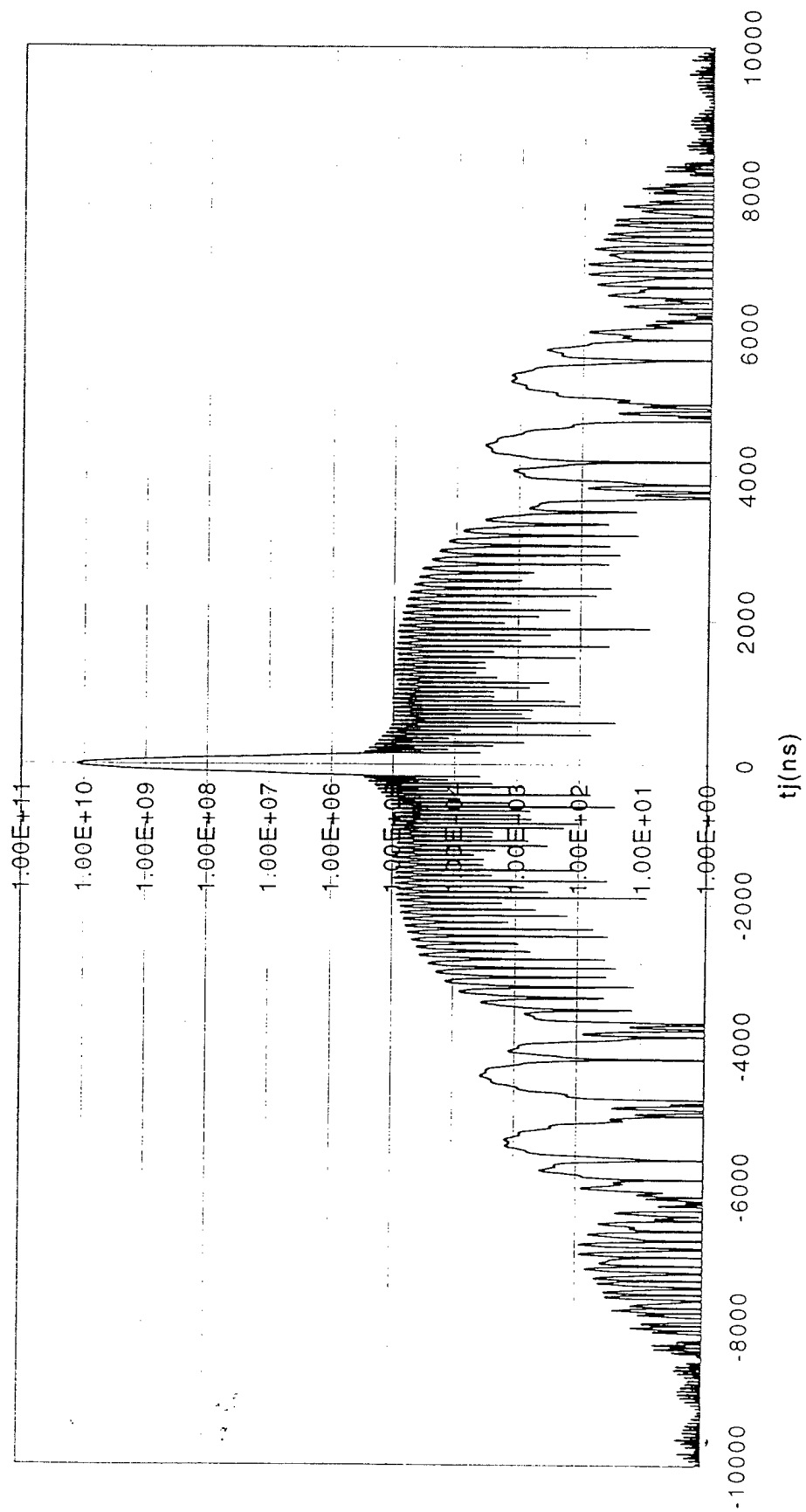
Figure 5. Filter response for the standard WARLOC pulse with the added Gaussian filter with f_G = 5 MHz and 200 ns rounded edge on both the transmitted pulse and the filter pulse.

$$\omega(t) = \omega' t + \alpha\omega' \frac{t}{\sqrt{1-(2t/\tau)^2}} \qquad (41)$$

The frequency becomes infinite at the pulse edges. Since the WARLOC radar is so constrained on receiver bandwidth, the nonlinear chirp does not appear to be an optimum use of the available bandwidth. Accordingly, at this point we do not look into the nonlinear chirp, but may do so in the future.

6. Enhanced Range Resolution with 'Stretch Processing'

In WARLOC, the transmitter will have considerably more bandwidth than the receiver. With stretch processing it is possible to obtain range resolution characteristic of the transmitter bandwidth, but only over a small distances from a central point. In theory, it is rather like range resolution with a cw fm radar. Imagine that the received pulse is given by Eq. (5), where now ω' is characteristic of the transmitter. For instance let us say that the transmitter bandwidth is 100 MHz in a 2.5 μs pulse, so that now $\omega' = 8\pi \times 10^{13}$ s^{-2}. If there is a single scatterer at range R, we find that the received signal is

$$\mathbb{R}_f(t) = \xi Q\left\{t - 2\left[\frac{R}{c}\right]\right\} \exp - i\omega'\left\{t - 2\left[\frac{R}{c}\right] - \frac{\tau}{2}\right\}^2 \equiv \xi \Xi\left(t - 2R/c\right) \qquad (42)$$

where we have neglected the velocity of the scatterer. Next multiply the filtered signal by the complex conjugate of the pulse Ξ^*, but centered at time t_0 to give a filter response which we define as N(t)

$$N(t) = \xi e^{i\psi} Q\left\{t - 2\left[\frac{R}{c}\right]\right\} Q\{t - t_0\} \exp 2i\omega'\left\{2\left[\frac{R}{c}\right] - t_0\right\}\left(t - \frac{\tau}{2}\right) \qquad (43)$$

where ψ is a phase dependent on the range. Notice that the frequency is proportional to the range and in fact is $2\omega'(2(R/c)-t_0)$. Thus the frequency of the filter is a measure of the range. However the maximum frequency is the receiver bandwidth, which we define as Ω, which is 40π MHz for WARLOC. Clearly, when using stretch processing, it is necessary for the low pass filter in the receiver to eliminate signals above 20 MHz, rather than alias them into the 0-20 MHz acceptance of the receiver. The WARLOC radar does in fact use a filter with very sudden drops at the edges of the 20 MHz resolution, so there is no aliasing from the higher frequency portion of the transmitted pulse. This gives a maximum range that R can be from the central point of

$$\left|\frac{2R}{c} - t_0\right|_{max} < \frac{\Omega}{2\omega'} \qquad (44)$$

Table 1

	3dB point (ns)	Integrated Sidelobes (-dB)	Efficiency
Matched filter:	48	9.3	1
Gaussian filter:			
$f_G = 5$ MHz	75	26.1	0.63
$f_G = 7.5$ MHz	60	21.0	0.84
$f_G = 10$ MHz	54	16.9	0.94

Performance characteristics of Gaussian filters of different frequency widths

Table 2

$T_r(T)$ ns	$T_r(F)$ ns	Integrated Sidelobes (-dB)
100	100	30.6
200	200	36
1000	1000	40
100	200	33

Sidelobe improvements with a Gaussian filter and rounded edges on the transmitted and/or filter pulses

Let us now look at the range resolution in the stretch processing mode. In a pulse of length τ, the frequency can be defined as long as the total phase shift is 2π or greater. Thus we get the range resolution in the stretch processing mode as

$$\Delta R = \frac{2\pi c}{2\omega'\tau} \qquad (45)$$

This is the standard expression for the range resolution of a radar whose bandwidth is the full bandwidth of the gyroklystron. For the example we have been using for WARLOC, the range resolution is 1.5 meters, and the total range which can be resolved is about 40 meters on either side of the central point.

Since the range resolution is given in terms of a frequency now, it is important that the Doppler shifts do not interfere with this measurement. The total phase shift from the Doppler effect if the particle velocity is v is $2v\omega\tau/c$, and this should be small compared to 2π. If the velocity is 10 m/s, the total phase shift is about 0.1 radian, which is small. Even if the pulse length were 10 μs instead of 2.5μs, the phase shift would still be small compared to 2π. However the droplet motion does put a constraint on pulse time for stretch processing.

Now let us quantify these concepts a little further. If the frequency can be resolved in units of $\omega_0 = 2\pi/\tau$, so that a frequency is specified by $n\omega_0$, let us define the Fourrier transform of N(n)

$$N(n) = \frac{1}{2\pi} \int_{-\infty}^{\infty} dt N(t) \exp in\omega_0 t \qquad (46)$$

Let us again consider the case of a 2.5 μs pulse with a linear frequency chirp extending from –50 MHz to 50 MHz. Since $f_0 = 4 \times 10^5 \ s^{-1}$, there are a total of 50 n values in Eq. (46) s the frequency goes from –10 MHz to 10 MHz. We define $t_0 = 0$ and then consider a target with some particular value of 2R/c. If 2R/c=0, the integral in Eq. (46) is proportional to a kroniker delta, $\delta_{n,0}$. Thus if the target is exactly centered in the range cell, there are no side lobes. However the target may not be exactly centered in the range cell. For instance we might have 2R/c=1ns. In this case the N(n≠0) ≠ 0, so there is a sidelobe issue. For the cloud radar, we are most interested in ambiguity from the distant sidelobes, so we define the performance of the radar in the following way. We start at the center of a range cell (say at 2R/c=0), that is the target is centered at the n=0 range cell. Then we consider the target uniformly distributed across the range cell, that is –2.5 ns < 2R/c < 2.5 ns. For the central lobe we consider n = -1,0 and +1 and sum over these. The sidelobes we consider a summation over all other n. Notice that we are defining the sidelobes so as to accept some ambiguity

between the central cell and its nearest neighbors. With this definition, we find that the integrated sidelobes are below the main lobe by about 11 db. That is, over the 75 meters or so which the radar examines, the significant variations in radar cross section must be less than a factor of about 10 for stretch processing to give a reasonably accurate image of the cloud at high range resolution.

References:

1. J.B. Mead, A. L. Pazmany, S. M. Sekelsky, and R. E. McIntosh: Proc. IEEE. 82, 1891, 1994
2. W. M. Manheimer, Int. J. Electronics, 72, 1165, 1993
3. W. M. Manheimer, Phys. Plasmas, 1, 1721, 1994
4. V. Gregers-Hansen, Private Communications, 1997-2001
5. M. Blank, B. Danly, B. Levush, P. Latham, and D. Pershing, Phys. Rev, Let. 79, 4485, 1997
6. B. Danly et al, IEEE Trans. Plasma Sci, 28, 713, 2000
7. M. Skolnik, Introduction to Radar Systems, 1980, McGraw Hill p 369
8. F. Ulaby, R. Morre, and A. Fung, Microwave Remote Sensing, Active and Passive, Volume II, Addison Wesley, 1982, p477-493
9. V. Gregers-Hansen, Intl. RAdar Symposium, IRS 98, 15-17 September, 1998, Munich Germany